Structural Optimization 11, 213–217 © Springer-Verlag 1996

Difficulties in truss topology optimization with stress, local buckling and system stability constraints

G.I.N. Rozvany

FB 10, Universität Essen, Postfach 103764, D-45117 Essen, Germany

Abstract A serious difficulty in topology optimization with only stress and *local* buckling constraints was pointed out recently by Zhou (1996a). Possibilities for avoiding this pitfall are (i) inclusion of system stability constraints and (ii) application of imperfections in the ground structure. However, it is shown in this study that the above modified procedures may also lead to erroneous solutions which cannot be avoided without changing the ground structure.

1 Introduction

Zhou (1996a) has shown that topology optimization of discretized trusses with only stress and local buckling constraints is rather meaningless for the following reasons.

- The supposedly "optimal" solution turns out to be unstable and hence for practical purposes useless, due to hinges along isolated compression members (with vanishing members in their neighbourhood).
- If we restore the stability of these solutions by hinge cancellations along such members, then their buckling length and the corresponding slenderness ratio increases, and hence the buckling stress decreases so drastically that this modified solution becomes highly nonoptimal.
- The actual (stable) optimal solution for the given ground structure looks entirely different from the above (unstable) optimal solution obtained for stress and member buckling constraints.

It seems reasonable to assume that such unstable optimal solutions can be avoided if *system stability constraints* are also added to the formulation. Another option for preventing solutions that are in stable equilibrium under the considered load only, is the introduction of *imperfections* into the ground structure. It will be shown, however, that even these modified formulations may lead to a nonoptimal solution.

2 Illustrative example

For computational simplicity and to improve clarity, we consider the elementary ground structure (Dorn *et al.* 1964) shown in Fig. 1a. If we impose only stress and local buckling constraints, then the solution in Fig. 1b is obtained, which is similar to Zhou's (1996a) result and is unstable. With a view to preventing such unstable solutions, the effect of system stability constraints is discussed in Section 3 (Appendix A) and the consequences of imperfections in Section 4 (Appendix B).

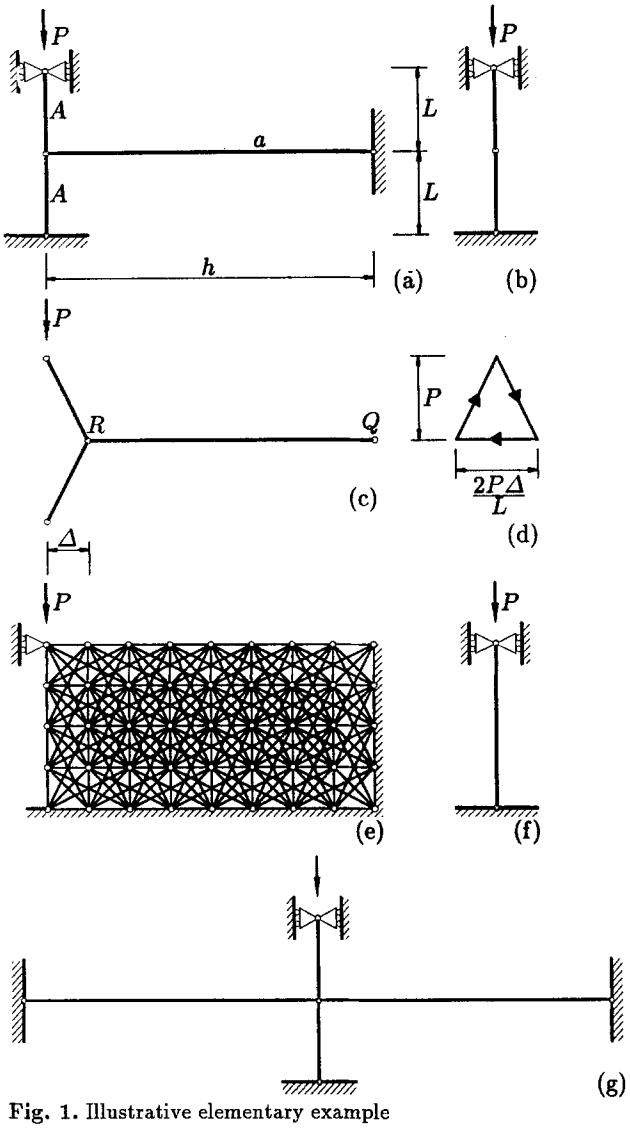

Fig. 1. Illustrative elementary example

3 Allowance for system stability

If additional system stability constraints are included, then the horizontal bar also takes on a nonzero cross-sectional area. This can be simply computed by considering the state of equilibrium for a small horizontal displacement at the inner joint (R in Fig. 1c). Details of this derivation and a numerical example are given in Appendix A.

It should be mentioned that realistic topology optimization problems would have a more complex ground structure (like the one in Fig. 1e), but these would be subject to the same difficulty.

We can conclude from the results in Appendix A that

- in the considered problem the inclusion of a *system stability constraint* indeed *gives a more economical solution* (Fig. 1a) *than the nominal optimal solution* (Fig. 1b) *with hinge cancellations for stability* (Fig. 1f).
- However, the *horizontal bar* turns out to be so *slender* that it would certainly buckle, before exerting a stabilizing effect on the system, in a real world situation.

To overcome this unrealistic design, one would have to introduce imperfections in the ground structure (see Section 4). This could be avoided only if the bracing system consisted of purely tensile members. Such a design is rarely possible in realistic problems, although in the considered example the ground structure could be modified in the manner shown in Fig. 1g, which would ensure that one of the horizontal bars is always in tension. This bar would stabilize the system even if it had the small cross-section obtained in the above example.

4 Use of imperfections to ensure stability of the nominal optimal solution

One of the doubtful features of the solutions in Section 3 is the fact that the horizontal bracing member is not subject to limitations by permissible or buckling stresses, because it is subject to a zero force until the vertical member buckles. A more realistic solution is obtained, which corresponds to current design philosophy, by introducing imperfections.

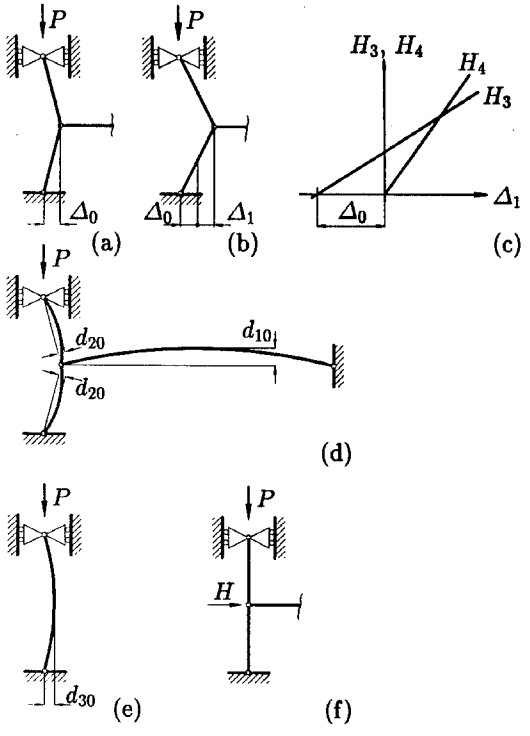

Fig. 2. Modified layout problem with imperfections

An example of such an imperfection Δ_0 is shown in Fig. 2a and the geometry, as well as the magnitude of the horizontal forces to be kept in equilibrium, under an additional horizontal displacement (Δ_1) in Figs. 2b and c.

Details of the derivation and a numerical example are given in Appendix B. The above results show that in the considered example the volume of the *solution with hinge cancellations* (Fig. 1f) *is significantly smaller than the one given by system stability* (Fig. 1a) *with imperfections for the original system.*

Note 1. Instead of considering Euler-buckling of the bars, an alternative, and more realistic, approach is to assume imperfections (curved bars with excentricities d_{10} and d_{20} in Fig. 2d and d_{30} in Fig. 2e) and then enforce permissible stress and stability conditions for these imperfect bars. However, this would not change significantly the conclusions of this paper.

Note 2. The introduction of another type of imperfection (small force in the horizontal direction at the joint, see Fig. 2f) would result in similar findings.

5 Concluding remarks

- The above examples show that even the introduction of *system stability constraints* and/or various types of *imperfections* in the original ground structure does not necessarily give the true optimal solution because some solution with *hinge cancellations* may have a lower weight.
- If we introduce *system stability constraints without imperfections*, then the solution without hinge cancellations (Fig. 1a) is nominally more economical (for realistic geometrical proportions) than the solution with hinge cancellation (Fig. 1f). However, the former is unrealistic because it does not allow for the instability of members required for bracing only. This is because these members are subject to zero forces, until buckling takes place.
- Once imperfections are introduced, *some solution with hinge cancelations* may be much more economical than the optimal solution for the original ground structure.
- It is *not practical* to locate systematically the *best structure with hinge cancellations* for large ground structures (used in topology optimization) because one would have to consider in a discrete procedure all combinations of hinge removals, which would be prohibitively expensive.
- Using some criterion for *hinge removal during an iterative procedure* may result in large errors because, once a hinge is removed, there exists no systematic method for reinserting it.
- The above results are *preliminary* ones and should be treated with caution, because they are based on *solid* (square) *cross-sections*, having partly very high slenderness ratios. The relative economy of solutions without hinge cancellation (but with system stability constraints and imperfections) is likely to be more favourable if *thin-walled* or *tubular cross-sections* are considered. These will be treated in a more detailed study.
- The long horizontal member (RQ in Fig. 1c) would be subject to substantial bending stresses due to *selfweight*, which should also be taken into consideration, unless some vertical suspension is provided. The effect of selfweight can be treated efficiently (e.g. Rozvany and Zhou 1992) by the DCOC method (Zhou and Rozvany 1992/93).

- The difficulties outlined by Zhou (1996a) and in this note also affect the topology (more correctly: "generalized shape") optimization of *perforated plates under plane stress*, which also results in very slender bar-like formations in compression. This can be seen in two examples given in Fig. 3. For the above reason, it is extremely important to treat the considered problems effectively in most branches of topology optimization.

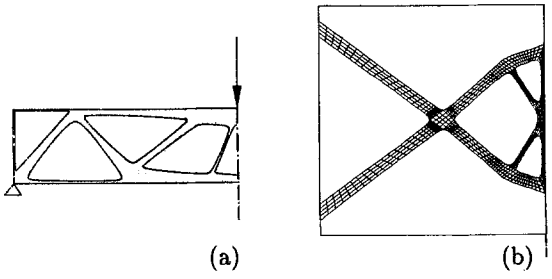

Fig. 3. Examples of generalized shape optimization of perforated plates under plane stress: (a) after Olhoff, Bendsøe and Rasmussen (1992); (b) after Rozvany *et al.* (1993)

- An additional difficulty with local buckling constraints is caused by *singular solutions* (Sved and Ginos 1968; Kirsch 1990; Cheng and Jiang 1992). These are due to the fact that, once a cross-sectional area becomes zero in an optimal solution, the permissible stress in the corresponding stress constraint jumps from a finite given value (the permissible stress σ_{p0} for tensile members) to infinity. The above problem becomes even more severe for compression members with buckling, because in that case the permissible stress jumps from a near-zero value (very slender members) to infinity (vanishing members). The relation between permissible stress (σ_p) and cross-sectional area (A) or member force (F) is shown graphically for tension and compression members, respectively, in Figs. 4a and b. A method for making the feasible set nonsingular was suggested by the author (Rozvany and Kirsch 1994), in which smooth envelope functions (broken lines in Fig. 4) replace the discontinuous functions for $\sigma_p(A)$. One such smooth function proposed was $\sigma_p = \sigma_{p0} \exp(A_0/A)$ where A_0 is a prescribed very small area value.
- The author and Zhou are working at present on *methods for overcoming the pitfalls* outlined in this paper. An important idea by Zhou for possible automatic hinge cancellation be discussed elsewhere (Zhou 1996b, Zhou and Rozvany 1996).

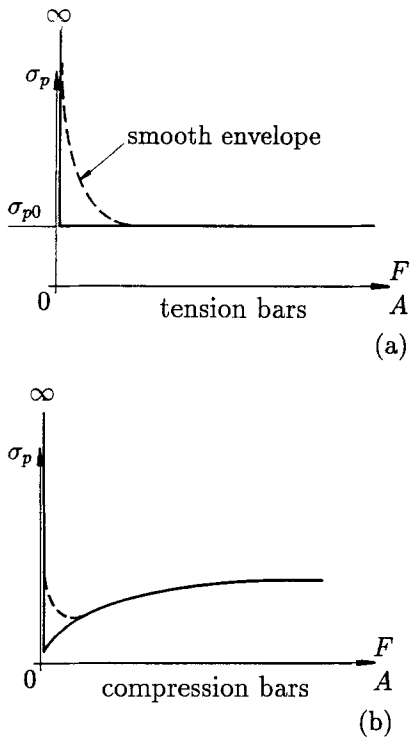

Fig. 4. The relation between permissible stresses (σ_p) and cross-sectional areas (A) or member forces (F) in topology optimization (continuous lines) and corresponding smooth envelope functions (broken lines)

Acknowledgements

The author is indebted to Dr. Zhou and to a referee of the paper for useful comments; to Karin Deutscher (text processing); to Elke Becker (drafting); and to Susann Rozvany (editing). The investigation presented herein has been prompted by Dr. Zhou's public discussions of papers at recent meetings. Financial support from the NATO Scientific and Environmental Affairs Division is also gratefully acknowledged, together with a fruitful exchange of ideas with Prof. Kaliszky (TU Budapest).

References

Cheng, K.-T.; Jiang, Z. 1992: Study on topology optimization with stress constraints. *Eng. Opt.* **20**, 129-148

Dorn, W.S.; Gomory, R.E.; Greenberg, H.J. 1964: Automatic design of optimal structures. *J. de Méchanique* **3**, 25-52

Kirsch, U. 1990: On singular topologies in structural design. *Struct. Optim.* **2**, 133-142

Olhoff, N.; Bendsøe, M.P.; Rasmussen, J. 1992: CAD-integrated structural topology and design optimization. In: Rozvany, G.I.N. (ed.) *Shape and layout optimization of structural systems and optimality criteria methods* (Proc. CISM Course held in Udine, 1990), pp. 171-197. Vienna: Springer

Rozvany, G.I.N.; Kirsch, U. 1994: Degenerate solutions in structural layout problems. Extended abstract submitted to *AIAA/NASA/USAF/ISSMO Symp. on Multidisciplinary Analysis and Optimization* (held in Panama City, Sept. 1994; the full paper was not presented due to restriction on the number of papers per author)

Rozvany, G.I.N.; Lewiński, T.; Sigmund, O.; Gerdes, D.; Birker, T. 1993: Optimal topology of trusses or perforated deep beams with rotational restraints at both ends. *Struct. Optim.* **5**, 268-270

Rozvany, G.I.N.; Zhou, M. 1992: Extension of new discretized optimality criteria methods to structures with passive control. *Proc. 4th AIAA/USAF/NASA/OAI Symp. on Multidisciplinary Analysis and Optimization* (held in Cleveland, OH), pp. 288-297. Washington D.C.: AIAA

Sved, G.; Ginos, Z. 1968: Structural optimization under multiple loading. *Int. J. Mech. Sci.* **10**, 803-805

Zhou, M. 1996a: Difficulties in truss topology optimization with stress and local buckling constraints. *Struct. Optim.* **11**, 134-136

Zhou, M. 1996b: Topology optimization of trusses subject to displacement, stress, local and system buckling constraints. Submitted to *19th Int. Congr. Theor. Appl. Mech.* (to be held in Kyoto, Japan)

Zhou, M.; Rozvany, G.I.N. 1992/93: DCOC: an optimality criteria method for large systems. Part I: theory. Part II: algorithm. *Struct. Optim.* **5**, 12-25; **6**, 250-262

Zhou, M.; Rozvany, G.I.N. 1996: Advances in overcoming computational pitfalls in topology optimization. Submitted to *6th AIAA/USAF/NASA/ISSMO Symp. on Multidisciplinary Analysis and Optimization* (to be held in Bellevue, WA)

Appendix A. Allowance for system stability

The horizontal force H_1 generated by moving the joint R in Fig. 1c horizontally by Δ is given by

$$H_1 = 2P\Delta/L\,, \tag{1}$$

(see Fig. 1d for the relevant force diagram). The same displacement generates a stabilizing force of

$$H_2 = \Delta Ea/h\,, \tag{2}$$

in the bar RQ, where E is Young's modulus for all bars, a the cross-sectional area of the horizontal bar and h its length. The system remains stable if the latter force is greater than the former, i.e.

$$H_2 - H_1 > 0\,. \tag{3}$$

The limiting case $H_2 - H_1 = 0$ then implies

$$2P\Delta/L = \Delta Ea/h\,, \tag{4}$$

giving

$$a = 2Ph/EL\,. \tag{5}$$

This means that the horizontal bar must take on at least the cross-sectional area in (5) for system stability.

A.1 Dimensioning of the vertical bars

We assume that the vertical bars are governed by Euler-buckling, for which the well-known critical force (F_k) and Euler stress (σ_e) are

$$F_k = \frac{\pi^2 EI}{L^2}\,, \quad \sigma_e = \frac{\pi^2 E}{\lambda^2}\,, \tag{6}$$

with

$$\lambda = \frac{L}{i}\,, \quad i = \sqrt{\frac{I}{A}}\,, \tag{7}$$

where I is the moment of inertia and A the area of the cross-section. Considering square cross-sections with a side length of d, we have

$$A = d^2\,, \quad I = d^4/12 = A^2/12\,, \quad i = d/\sqrt{12}\,,$$

$$F_k = \frac{\pi^2 EA^2}{12L^2}\,, \quad \sigma_e = \frac{\pi^2 EI}{L^2 A} = \frac{\pi^2 EA}{12L^2}\,. \tag{8}$$

Then the area requirement A for a given axial force P becomes

$$A = \frac{L}{\pi}\sqrt{\frac{12P}{E}}\,. \tag{9}$$

A.2 Check on the optimality of the considered layout (Fig. 1a)

It follows from (5) and (9) that the total truss volume becomes

$$V_1 = \frac{2L^2}{\pi}\sqrt{\frac{12P}{E}} + \frac{2h^2 P}{LE}\,. \tag{10}$$

Considering the modified solution with a longer vertical bar without a hinge (Fig. 1f), we have by (9) with $L \to 2L$

$$A_2 = \frac{2L}{\pi}\sqrt{\frac{12P}{E}}\,, \quad V_2 = \frac{4L^2}{\pi}\sqrt{\frac{12P}{E}}\,. \tag{11}$$

Clearly, the second solution is more economical if

$$\frac{2L^2}{\pi}\sqrt{\frac{12P}{E}} < \frac{2h^2 P}{LE}\,, \tag{12}$$

or

$$\frac{12L^6 E}{P\pi^2 h^4} < 1\,. \tag{13}$$

This means that for large values of h/L and/or P/EL^2 the solution in Fig. 1f is optimal and hence even an additional system stability constraint without hinge cancellation would yield a nonoptimal solution.

A.3 Consideration of additional permissible stress (e.g. yield stress) constraints

For low slenderness ratios (i.e. for large compressive member forces), the permissible (or yield) stress σ_p has a lower value than the Euler buckling stress (σ_e). This is shown in Fig. 5, which represents graphically the cross-sectional area A/force F relation for a typical truss element. If the permissible stress governs the design, then the cross-sectional area of the vertical members becomes

$$A = \frac{P}{\sigma_p}\,, \tag{14}$$

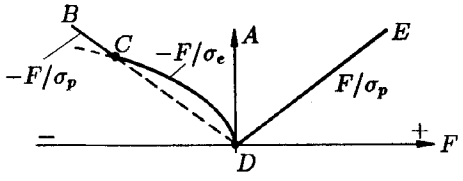

Fig. 5. Cross-sectional area/member force relation for trusses

and the corresponding total volume

$$V_3 = \frac{2LP}{\sigma_p} + \frac{2h^2 P}{LE}\,. \tag{15}$$

If the bar in Fig. 1f is still governed by the Euler stress, then

$$V_3 < V_2\,, \tag{16}$$

with (11) and (15) implies that the solution in Fig. 1f is optimal. However, if the bar in Fig. 1f is also governed by the permissible stress constraint, then the total volume becomes

$$V_4 = \frac{2LP}{\sigma_p}\,. \tag{17}$$

This is always lower than V_3 in (15) and hence the solution in Fig. 1f is optimal.

A.4 Numerical example

Consider the problem in Fig. 1a with $P = 200$ kN, $L = 3$ m, $E = 210000$ N/mm^2 and $\sigma_p = 240$ N/mm^2. The material properties are given by the relevant German design standard (DIN 18800 for the steel St 37). Then the limiting case for (13) gives

$$h = \frac{1}{1000}\left(\frac{12 \times 3000^6 \times 210000}{\pi^2 \times 200000}\right)^{1/4} = 174.66\,\text{m}, \qquad (18)$$

which is well outside the realm of practical structures. For shorter horizontal bars (with $h < 174.66$ m), the layout in Fig. 1a is more economical than the one in Fig. 1f. The cross-sectional area for the vertical member by (9) would become

$$A = \frac{3000}{\pi}\sqrt{\frac{12 \times 200000}{210000}} = 3228.25\,\text{mm}^2 \qquad (19)$$

and the corresponding stress

$$\sigma = \frac{200000}{3228.25} = 61.953\,\text{N/mm}^2,$$

which is much smaller than the permissible (yield) stress of 240 N/mm^2. Taking a realistic value for h by adopting $h = 12$ m, (5) gives for the cross-sectional area the horizontal bar

$$a = \frac{2 \times 200000 \times 12000}{210000 \times 3000} = 7.62\,\text{mm}^2. \qquad (20)$$

Appendix B. Modified truss with imperfection

Assuming a *small* initial horizontal imperfection Δ_0 at the joint (Fig. 2a), we have a force H_0 in the horizontal member

$$H_0 = \frac{2\Delta_0 P}{L}. \qquad (21)$$

For an additional displacement of Δ_1 (Fig. 2b), we have the horizontal force

$$H_3 = \frac{2(\Delta_0 + \Delta_1)P}{L}. \qquad (22)$$

The stabilizing force generated by strains in the horizontal member becomes

$$H_4 = \Delta_1 Ea/h. \qquad (23)$$

The forces H_3 and H_4 are shown graphically in Fig. 2c. Equilibrium is reached if

$$H_3 = H_4, \qquad (24)$$

implying

$$\Delta_1 = \frac{2\Delta_0 Ph}{EaL - 2Ph}. \qquad (25)$$

Received Jan. 5, 1996
Revised manuscript received March 14, 1996

The result in (25) assumes that the lines representing H_3 and H_4 in Fig. 3c do intersect for $\Delta_1 > 0$, which implies the additional condition for stability

$$\frac{Ea}{h} > \frac{2P}{L} \quad \text{or} \quad a > \frac{2Ph}{EL}. \qquad (26)$$

For a given value of "a", Δ_1 can be calculated from (25) and then H_3 from (22). Then "a" must also satisfy the conditions

$$a \geq \frac{H_3}{\sigma_p} \quad \text{and} \quad a \geq \frac{H_3}{\sigma_e}. \qquad (27)$$

Considering the solution with hinge cancellation (Fig. 1f), the cross-sectional area A must satisfy the conditions

$$A \geq \frac{P}{\sigma_p} \quad \text{and} \quad A \geq \frac{P}{\sigma_e}. \qquad (28)$$

B.1 Numerical example

We consider again the problem in Fig. 1a with $P = 200$ kN, $L = 3$ m, $E = 210000$ N/mm^2, $h = 20$ m and $\sigma_p = 240$ N/mm^2. The imperfection Δ_0 in Fig. 2a will be assigned the value $\Delta_0 = 30$ mm (which is 0.5% of the combined length of the vertical members). The relevant equations on the basis of (25), (22) and a modified version of (9) are

$$\Delta_1 = \frac{2\Delta_0 Ph}{EaL - 2Ph}, \quad H_3 = \frac{2(\Delta_0 + \Delta_1)P}{L},$$

$$a = \frac{h}{\pi}\sqrt{\frac{12H_3}{E}}, \qquad (29)$$

giving the values

$$\Delta_1 = 0.12542543\,\text{mm}, \quad H_3 = 4016.72339\,\text{N},$$

$$a = 3049.9804\,\text{mm}^2, \qquad (30)$$

or

$$\sigma = 1.316967\,\text{N/mm}^2. \qquad (31)$$

The latter agrees with the Euler-stress σ_e given by (8). The above stress value is considerably smaller than the yield stress ($\sigma_p = 240$ N/mm^2).

By (19) and (30), the total volume of this design is

$$V_1 = 3228.25 \times 6000 + 3049.98 \times 20000 = 80369100\,\text{mm}^3. \qquad (32)$$

For the solution with hinge cancellation (Fig. 1f), (11) gives

$$V_2 = 38739017\,\text{mm}^3, \qquad (33)$$

which is less than half of the nominal optimal solution for the original ground structure with imperfections.